Control of an ultrasonic haptic interface for button simulation

Pierre Garcia, Frédéric Giraud, Betty Semail, Matthieu Rupin, Anis Kaci

Control of an Ultrasonic Haptic Interface for Button Simulation

Pierre Garcia[a,b], Frédéric Giraud[b], Betty Lemaire-Semail[b], Matthieu Rupin[a], Anis Kaci[b]

[a] *Hap2u, 75 avenue Gabriel Péri, 38400 Saint-Martin-d'Hères*
[b] *Univ. Lille, Centrale Lille, Arts et Metiers Institute of Technology, Junia, ULR 2697 L2EP -F-59000 Lille, France*

Abstract

This work presents the control of a piezoelectric interface that combines two vibration modes of a plate to render the haptic feeling of a button click. By principle, the two vibration modes create an elliptical motion of particles of a beam that can induce a lateral force to the fingerpulp. In this device, the synchronization of the modes' vibrations is essential, and can be obtained with a closed loop control. In the paper, we present the control in the (d,q) frame, because it can ensure the dynamic performances to achieve a compelling haptic feedback, yet being robust besides the external disturbances produced by the user's finger. The proposed method could achieve a 2ms response time, and the haptic feedback was perceived by 100% of users in a psychophysical study.

Keywords: Haptic, piezoelectric, tactile

1. Introduction

Touchscreens are convenient and cost effective input devices, and they have replaced the physical knobs and buttons in most of consumer products. However, they only provide to users a visual feedback, and the fact that the touched surface remains hard and flat reduces their acceptability. This is why, researchers have devised ways to introduce more haptic feedback on touchscreens [1], leading to haptic surfaces.

To create the illusion of touching a button while pressing on a flat screen, it has been proposed to make the plate vibrate at low frequency, in order to produce in the finger pulp a deformation that is perceived as a click [2, 3, 4]. However, due to the low frequency used, an audible noise is emitted in the same time as the stimulation is produced which can be disturbing for the user. To avoid this problem, ultrasonic vibration of a plate can be used [5]. Indeed, when pressing on a plate with a finger, internal stresses increase with the normal force. Above a force threshold, the plate is put in vibration,which instantaneously decreases the friction with the fingerpulp and releases the aforementioned stresses. This rapid transition between the two states of the finger pulp is perceived as a

button click. Moreover, in order to reduce the detection threshold of click recognition, the internal stresses can be increased thanks to lateral forces generated by ultrasonic vibrations [6]. Indeed, if specific conditions are met, particles on the surface of a vibrating plate undergo an elliptical motion which is capable of producing these lateral forces even with a stationary finger [7].

The device presented in this paper derives from [8]. It consists in a beam which dimension is precisely adjusted in order to have one bending mode and one longitudinal mode at the same frequency, and energized by piezoelectric patches. The bending mode produces a displacement of the particles w_B along a vertical axis, while the longitudinal mode produces a linear and horizontal displacement w_L. When the two vibration modes are excited simultaneously at the same frequency, but with a phase shift of $\pm\pi/2$ an elliptical motion occurs, producing the net lateral force, as described figure 1. Previous research has shown that optimal haptic feedback is produced when the displacements along the two directions are equal [8].

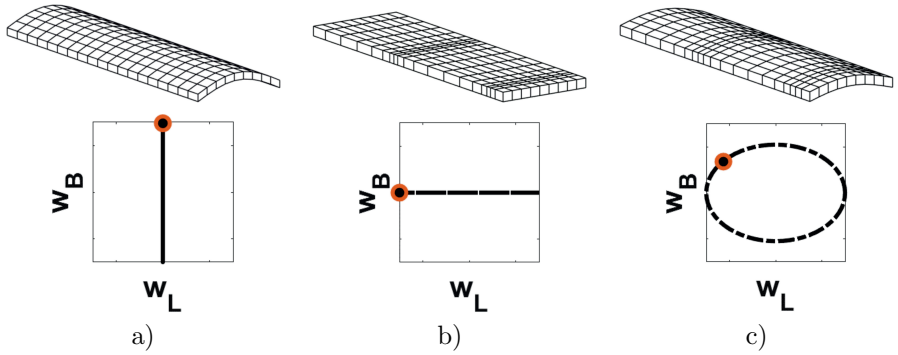

Figure 1: Vibration mode (top) and corresponding displacement of the point at the top surface (bottom) for a) bending, b) longitudinal and c) superposition of the two modes

However, fulfilling the conditions for an elliptical motion of the particles is not an easy task. Indeed, adjusting the prototype's dimension to guarantee a perfect match of the two modes' resonant frequencies is practically impossible due to the precision of manufacturing. Moreover, external disturbances, and principally the fingertip that acts as a mechanical impedance for the vibration, can move the vibration away from the optimal condition for haptic. Fortunately, dimension discrepancies and disturbances can be compensated by tuning the electrical supply conditions of the piezoelectric patches. In particular [9] uses an optimization algorithm, but it is not shown to be robust besides perturbation. To cope for this issue, [10] proposes a closed loop control to automatically adjust the voltages in phase and amplitude.

In this paper, we applied the closed loop control in order to synchronize two vibration modes which resonance frequency are not equal. First, a dynamic model of the vibration is presented, then the controller is designed based on this model. Finally, experimental results are presented.

2. System's description

2.1. Presentation of the system

Our prototype consists of a 148 x 18 x 2 mm^3 aluminium plate, actuated by nine piezoelectric ceramic actuators in total (5 mm x 7 mm x 0.5 mm from Noliac, Denmark) with two additional ceramic plates used as sensors (14 mm x 2 mm x 0.3 mm, Noliac Denmark), and is depicted figure 2. The bounding conditions are free, which is practically obtained by placing the plate on a specific foam chosen to not modify its vibration. The bending and longitudinal modes

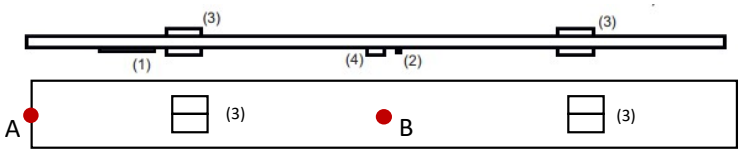

Figure 2: View of the plate with (1) longitudinal sensor, (2) bending sensor,(3) longitudinal actuators,(4) bending actuators; A and B are location of laser spot for sensors calibration.

chosen to be combined in order to produce the elliptical motion of particles, was found to be close in frequency on our prototype, with a resonance frequency of 34100Hz and 34250Hz respectively. Their deformed shapes are presented figure 3.

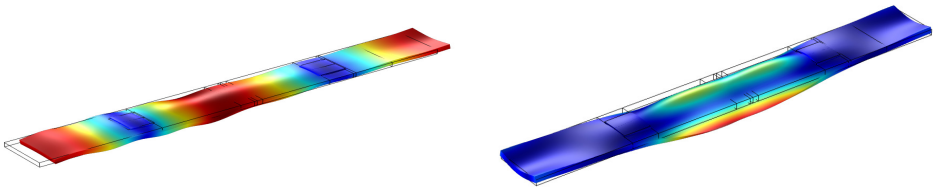

a) b)

Figure 3: Modal shape of the beam equipped with piezoelectric actuators obtianed with a FEM simulation on Comsol multiphysics; a) longitudinal b) bending modes

A calibration of the two sensors has been carried out with a laser interferometer. The location of the measurement spots was place in the middle of the plate (point A on figure 2) to calibrate the bending mode sensor, and on the plate's edge (point B on figure 2) for the longitudinal mode. The frequency response of the plate is presented in figure 4; the resonant frequency of the bending mode is $34100Hz$ and of the longitudinal one is $34250Hz$. The difference between the resonant frequencies seems small ($\approx 150Hz$ or 0.4%), but since their bandwidths are small due to high quality factors, one mode falls outside of the bandwidth of the other one, which leads us to work at an intermediate frequency ($f = 34.2kHz$).

If the intermediate frequency is adequately chosen, then the required operating point (the 2 modes having the same vibration amplitude with a phase shift

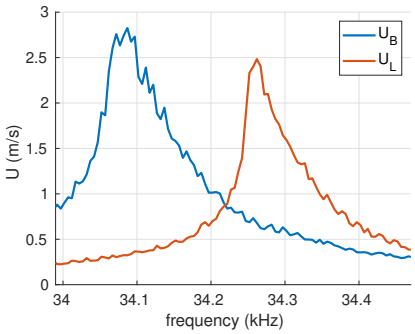

Figure 4: Frequency response of the vibration speed for each mode; U_B is the vibration speed for the bending mode and U_L is for the longitudinal mode

of $\pm\frac{\pi}{2}$) can be obtained by imposing two voltages, also with the same amplitude and in quadrature. However, the resonance frequencies of the system vary with external factors, like temperature for instance. In this paper, we decided to focus on the real-time control of the amplitudes and phases of the vibration modes, without taking into account the frequency tracking. Indeed, the variation of frequencies can be compensated, to some extent, by the driving voltages. For that purpose, a model of the system is given in the next section.

2.2. Model projection in the (d,q) coordinate system

We consider a plate, which length is L, thickness b and height H. The displacement of the bending mode is denoted w_B, obtained when the bending mode actuator is supplied with a voltage v_B. In the same way, we define w_L and v_L the displacement and the voltage for the longitudinal mode. All along the paper, we assume that the system is linear, so the two modes are not coupled, yielding to the following lumped parameters model of equations 1 and 2:

$$M_B\ddot{w_B} + D_B\dot{w_B} + K_B w_B = N_B v_B \tag{1}$$

$$M_L\ddot{w_L} + D_L\dot{w_L} + K_L w_L = N_L v_L \tag{2}$$

With M_B and M_L the modal mass, K_B and K_L the modal stiffness, D_B and D_L the modal damping and N_B and N_L the force factors of the bending and longitudinal modes respectively [10]. Moreover, the resonance frequencies f_{B0} and f_{L0} for the two modes are given by:

$$f_{B0} = \frac{1}{2\pi}\omega_{B0} = \frac{1}{2\pi}\sqrt{\frac{K_B}{M_B}} \quad \text{and} \quad f_{L0} = \frac{1}{2\pi}\omega_{L0} = \frac{1}{2\pi}\sqrt{\frac{K_L}{M_L}} \tag{3}$$

In steady state, the displacements are sinusoidal functions of time, while their amplitude and phase are constant. Therefore, as it is done with modern

electromagnetic motors, we use complex phasor to change the system with invariant variable in steady state. We then introduce the complex phasor writing $x(t) = \Im(\underline{x})$ with :

$$\underline{x} = \underline{X} e^{j\omega t} \tag{4}$$

where $\underline{X}$ is the complex amplitude, which describes the amplitude and the phase of $x(t)$, and $\omega/2\pi$ the frequency of the vibration. Hence, $\underline{x}$ is equivalent to a rotating vector that is projected onto a rotating reference frame; as a result, in steady state, $\underline{X}$ is a constant. For sake of clarity, a new orthogonal reference frame denoted by (d,q) is defined, such that the axis d is aligned with $e^{j\omega t}$. We define then X_d and X_q as the projection of $\underline{X}$ on axes d and q:

$$\underline{x} = (X_d + jX_q)e^{j\omega t} \tag{5}$$

By applying the projection to w_B,w_L,v_B and v_L we obtain :

$$\begin{aligned} \underline{w_B} &= (W_{Bd} + jW_{Bq})e^{j\omega t} \qquad \underline{w_L} = (W_{Ld} + jW_{Lq})e^{j\omega t} \\ \underline{v_B} &= (V_{Bd} + jV_{Bq})e^{j\omega t} \qquad \underline{v_L} = (V_{Ld} + jV_{Lq})e^{j\omega t} \end{aligned} \tag{6}$$

For the purpose of conciseness, we introduce the vibration velocity $u(t) = \dot{w}$, and its complex phasor $\underline{u} = (U_d + jU_q)e^{j\omega t}$. Moreover, due to the high quality factor generally admitted for the device, several assumptions can be made:

- The frequency of the voltage varies slowly, and we consider $\dot{\omega} = 0$,
- The dynamic of the vibration amplitude is slow compared with the derivative of the vibration, and $\ddot{W}_{d,q} \approx 0$.

Under these assumptions, the equation 1 and 2 become four equations, one for each mode and each axis:

$$\begin{cases} NV_{id} = (M + \frac{K}{\omega^2})\dot{U}_{id} + DU_{id} + (\frac{K}{\omega} - M\omega)U_{iq}, \\ NV_{iq} = (M + \frac{K}{\omega^2})\dot{U}_{iq} + DU_{iq} - (\frac{K}{\omega} - M\omega)U_{id}. \end{cases} \tag{7}$$

With $i = \{B, L\}$ respectively for the bending and longitudinal mode, which remains valid in the remaining of this paper.

These equations are the model in the rotating frame. In order to simplify this model, we consider that ω is close to the value at resonance, and we introduce then $\delta\omega_i$ the deviation from ω_{i0} to ω, $\omega = \omega_{i0} + \delta\omega_i$ with $\delta\omega_i \ll \omega_{i0}$. We can then consider $M_i + \frac{K_i}{\omega^2} \approx 2M_i$ and $\frac{K_i}{\omega} - M_i\omega = 2M_i\delta\omega_i$, leading the simplified equations (8):

$$\begin{cases} N_i V_{id} = 2M_i\dot{U_{id}} + D_i U_{id} - 2M_i\delta\omega_i U_{iq} \\ N_i V_{iq} = 2M_i\dot{U_{iq}} + D_i U_{iq} + 2M_i\delta\omega_i U_{id} \end{cases} \tag{8}$$

These equations represent the dynamic model of the piezoelectric actuators in the dq frame. In this model, the vibration amplitude behaves like a first order type differential equation on each axis, with a cross coupling. They are first exploited at steady state in order to identify the modal parameters of the system.

2.3. Modal parameters identification

Considering steady state operation will help us to identify the system's parameters. In this condition, the derivatives of U_d and U_q are equal to 0. Moreover, during this operation, the voltage is imposed by an external electronic circuit, and we assume that $V_{id} = V$ and $V_{iq} = 0$; the equations 8 lead to:

$$\begin{cases} D_i U_{id} - 2M_i \delta\omega_i U_{iq} = N_i V \\ D_i U_{iq} + 2M_i \delta\omega_i U_{id} = 0 \end{cases} \tag{9}$$

From Eq.(9), we found that if $U_q = 0$ then $U_d = 0$; otherwise, we have :

$$2M_i \delta\omega_i = D\frac{U_q}{U_q} \tag{10}$$

By injecting the equation (10) into (9) we can eliminate $2M_i\delta\omega_i$, which eventually leads to the equations (11):

$$U_{qB}^2 + (U_{dB} - \frac{N_L V_B}{2D_B})^2 = (\frac{N_B V_B}{2D_B})^2 \qquad U_{qL}^2 + (U_{dL} - \frac{N_L V_L}{2D_L})^2 = (\frac{N_L V_L}{2D_L})^2 \tag{11}$$

Hence, when sweeping ω from below to above the resonance, $\underline{U_i}$ follows a circle, centered on $(\frac{N_i V}{2D_i}, 0)$, and which radius equals to $\frac{N_i V}{2D_i}$. Moreover, It can be shown that the system's bandwidth f_{iBP} is a function of M_i and D_i with:

$$f_{iBP} = \frac{1}{2\pi}\frac{D_i}{M_i} \tag{12}$$

Hence, to identify our prototype's parameters, we energized each mode successively, by sweeping ω from 34 to 34.48 kHz, with $V = 60V$. Plotting U_q as a function of U_d we obtain the figure 5.

In figure 5, we also depicted the interpolated circle obtained from the experimental data. It can be seen that the model presented in the equations 12 is consistent with the measurements. By measuring the radius of each circle and the system's bandwidth, we obtain the following identified parameters: $\omega_{BP_B} = 440 rad/s$, $\omega_{BP_L} = 377 rad/s$, $\frac{N_B V_B}{2D_B} = 1.4 m/s$, $\frac{N_L V_L}{2D_L} = 1.2 m/s$.

In order to verify the parameters identified from the circle, we compare the simulated and measured transitory response of U_d to a step variation of V_d at resonance ($\delta\omega = 0$) and for each mode. As it can be seen figure 6, the measures validate the model's output, hence confirming the approach detailed in this section. The open loop response time observed on this figure is $8ms$ for the bending mode and $7ms$ for the longitudinal mode.

Based on the system's model in the rotating reference frame, a controller is designed and presented in the next section of this paper.

3. closed loop control of the the vibration

3.1. Controller design

In the rotating reference frame, each axis of each mode is controlled. For instance, in order to have two modes vibrating at the same frequency with a

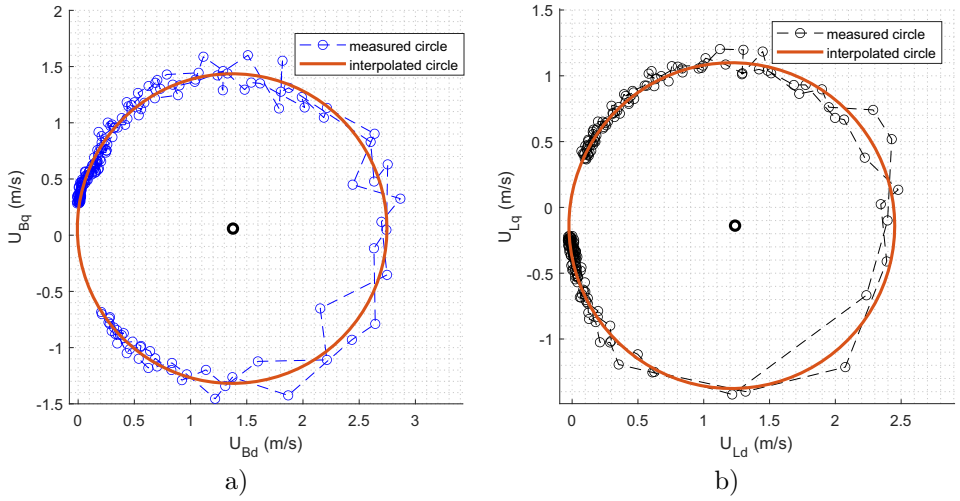

Figure 5: Measured (dash line) and interpolated circle in the rotating reference frame used for the identification of the parameters for a) the bending mode and b) the longitudinal mode

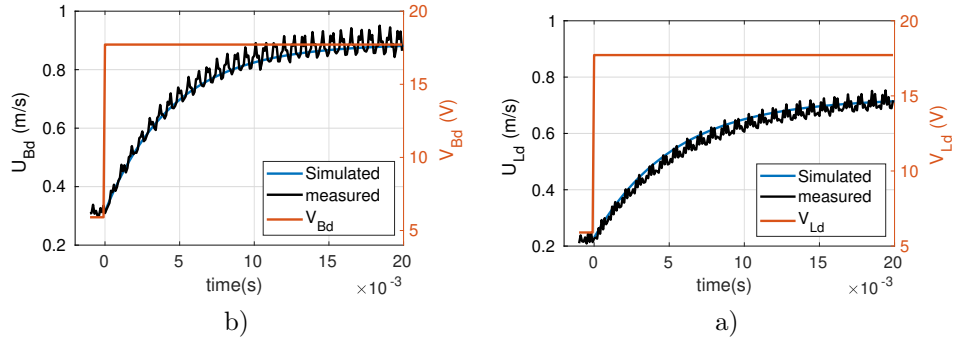

Figure 6: Measured and simulated step response at the resonant of the system for a) the bending mode and b) the longitudinal mode.

phase shift of $\pi/2$, the reference set points can be as follows: $U_{Ld} = U_{Bq} = U$, $U_{Lq} = U_{Bd} = 0$. In closed loop, the voltages applied to the actuators are automatically adjusted in order to attain these references, no matter whether the operating frequency is close to one mode or an other. The block diagram of the control loop in the axis d is given figure 7. In this figure, the transfer function of the system is extracted from the equation 8 after applying the Laplace transform, which leads to:

$$\frac{U_i d}{V_i d} = \frac{N_i}{2M_i s + D_i} = \frac{\frac{N_i}{D_i}}{2\frac{M_i}{D_i}s + 1} \tag{13}$$

In the remaining of the paper, we design the controller for the axis d, but

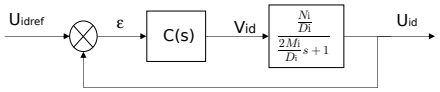

Figure 7: Block diagram for the control of the two modes along the axis d and q.

the same methodology can be followed for the other axis. Since the system's transfer function of the equation 13 shows a single pole at $\omega_1 = \frac{Di}{2M_i}$, we choose for $C(p)$ a PI controller, such that:

$$C(s) = K_P + \frac{K_I}{s} \tag{14}$$

The controller is designed in order to compensate the pole ω_1 and to ensure a closed loop response time denoted t_r; we have then :

$$K_P = \frac{3D_i \frac{2M_i}{D_i}}{tr} \qquad K_I = \frac{2M_i}{D_i} \times K_p \tag{15}$$

The controller is implemented for each mode (L and B) and each axis (d and q) in a DSP (STM32F405 from ST Microelectronics), for a response time $t_r = 2ms$. The sampling period is equal to $100\mu s$.

The performances of the control loop are presented in the next section.

3.2. Experimental results

To assess the performances of the control loop, we first test its performance at the resonant frequency($\delta\omega = 0$). For that purpose we use a step for U_{Bdref} while U_{Bqref} remains equal to 0; the same is done for the longitudinal mode. The transitory step responses are presented in figure 8.

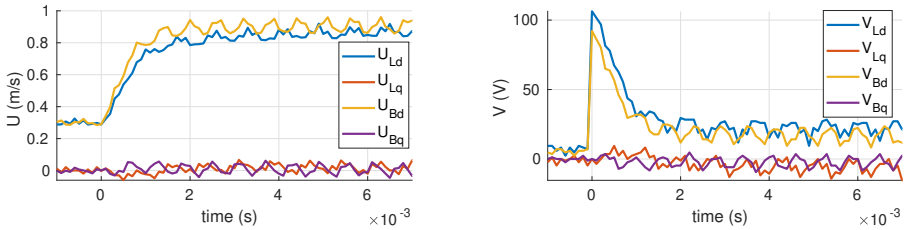

a) b)

Figure 8: Experimental results of the closed loop control at the resonant frequency for the bending modes and the lateral mode; a) vibration speed and b) supply voltage. Each mode is tested independently of the other, at it resonance frequency.

The figure 8 shows a response time equal to $2ms$, with no overshoot or static error, as expected from the design requirements of $C(s)$. Hence, the system is faster in closed loop than in open-loop. To obtain this performance, the voltage shows a spike at $t = 0$ (around 100V) before stabilizing around a lower value

(20V) in steady state. Moreover, since the system is operated at the resonance for each mode, the coupling between the axis d and q vanishes, and $V_{Lq} = 0$ in order to have $U_{Lq} = 0$ as expected from the equation 8.

The system is then operated at a frequency between the two resonance frequency ($\delta\omega \neq 0$), while the references for U_{id} and U_{iq} remain equal as in the last try. The results are presented figure 9.

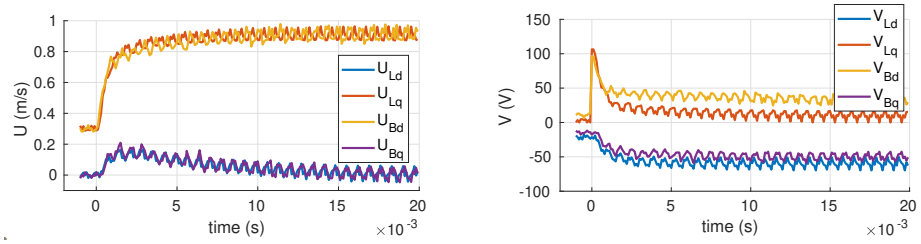

a) b)

Figure 9: Experimental results obtained at $\delta\omega \neq 0$ a) vibration speed and b) supply voltage. During the test, both modes are energized.

The figure 9 shows that the system's response time is approximately $6ms$. Indeed, the couplings that exist between the axis d and q have to be compensated by the controller, and it takes more time. As a result, the component of the voltage V_{Lq} is not equal to 0, and needs to be adapted to compensate these couplings. Indeed, at the resonance of each mode successively, V_{Bq} and V_{Ld} equal 0 when $U_{Bq} = U_{Ld} = 0$. Outside the resonance, the couplings need to be compensated, so the voltage needs to be adapted in amplitude and phase to maintain the vibration to the reference setpoint. This can be depicted by the figure 10, which presents the vibration speeds U_B and U_L as well as the voltages V_B and V_L in the rotating reference frame and for the steady state of figure 9: at resonance, the voltages would have been along axis d and q for V_B and V_L respectively, but we can observe that they were rotated.

To create the illusion of a button click, the direction of the elliptical motion needs to be inverted during the pressing movement of the user. To achieve this, the sign of U_{Bq} is invert while keeping the other references constant. The transitory responses are presented figure 11, where we inverse the motion direction at $t = 0$. In this example, the response time is $2ms$, without any overshoot or static error.

The same test is presented with a finger pressing on the beam. The results also presented figure 11 show that to obtain the same vibration velocity as without a finger, the voltage V_{Bq} needs to be increased. Indeed, the fingerpulp acts as a mechanical impedance, that needs to be compensated. Again, this is automatically achieved, by the closed loop control; therefore, robustness besides the perturbation of the finger in demonstrated.

Hence, thanks to the closed loop control, the conditions to simulate a button click in our system are guaranteed. We then conduct a psychophysical study to assess the performances on several participants.

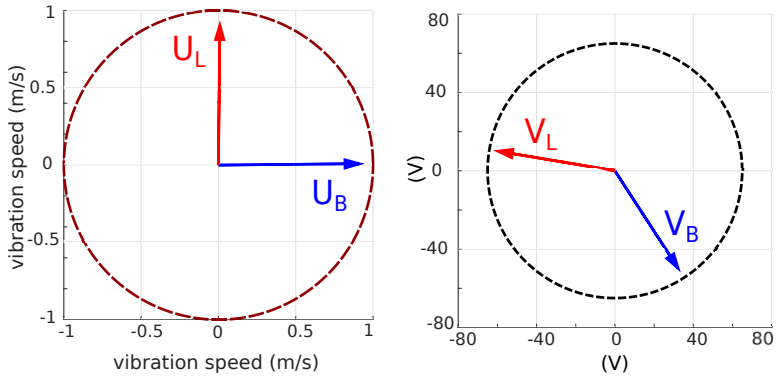

Figure 10: Vectors of a) the vibration speed and b) the voltage in the (d,q) reference frame, when the device is operated between the two modes resonance frequencies.

4. Psycho-physical study

For the experiment, the plate is mounted on a force sensor that measures the normal force exerted by the user on the plate. Three conditions are defined: the condition $C1$ simulates a click with the elliptical motion of particles; the condition $C2$ simulates a click with the bending mode only, so there is no elliptical motion of the particles; in the condition $C0$, no stimulation is produced, and acts as a control condition.

The key click simulation for $C1$ was performed as follows; two normal force thresholds were defined $f_1 = 0.4N$ and $f_2 = f_1 + 0.3N$. When the user reaches f_1, we turn on the two modes, with specific vibration speeds U_L and U_B. When f_2 is reached, the direction of the elliptical motion is reversed simply by inverting U_B. At the end, when the user releases his finger from the surface, we turn off the device. For the condition $C2$ the device is switched on at f_2, and switched of when the user releases his finger.

Data were collected from ten volunteers aged between 18 and 40. Participants were wearing noise-cancelling headphones in order to prevent noise disturbance. All participants gave written informed consent. The investigation is conformed to the principles of the Declaration of Helsinki and experiments were performed in accordance with relevant guidelines and regulations.

The force is sampled at 10kHz by the DSP, and a Laptop PC is used to send the threshold value f_1 and the amplitude set points U_B and U_L to the DSP through USB.

After a training period during when participants could discover the haptic feedback,they had to press once on the middle of the plate with their index finger. They were asked whether or not they could feel the virtual key click. The condition were randomized to avoid the prediction effect. The experiment ended when all condition are presented 10 times.

For all conditions, we have computed the median success rate, and the stan-

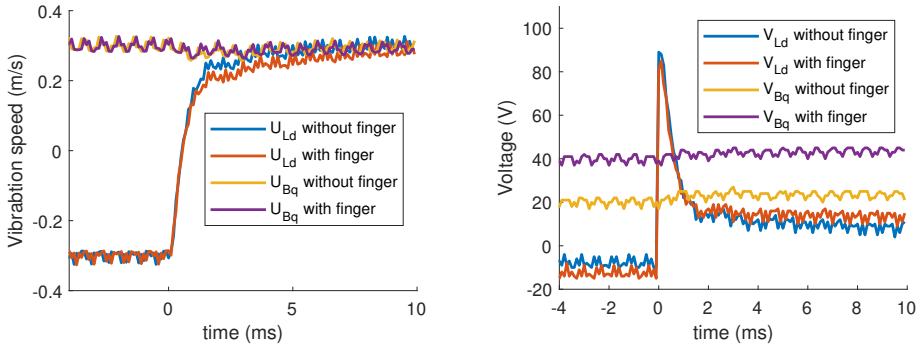

Figure 11: Transitory response of a) the vibration speed and b) voltage when reversing the direction of the elliptical motion of the particles, with $U_{Ld} = \pm U_{Bq} = 0.3m/s$. In this figure, the results are presented with or without a finger on the beam.

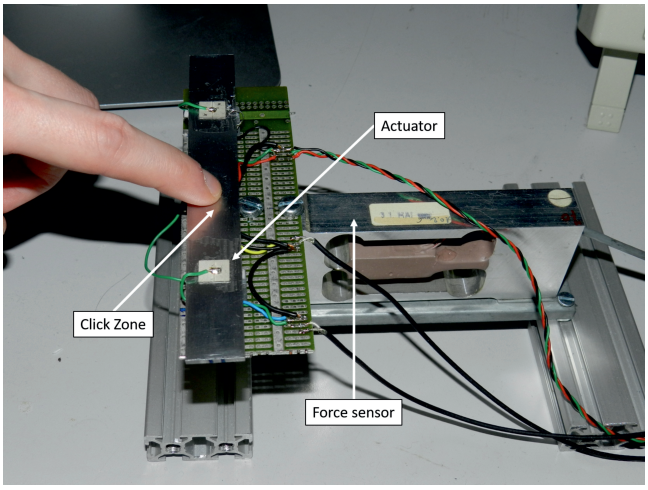

Figure 12: The device used for the psychophysical study

dard deviation (Std) which are presented figure 13 and in Table 1. The result shows very different success rate depending on the condition. When the stimulation is created only from normal displacement of the surface, the success rate is only 30% with a large Standard deviation (19%). This confirms the study in [8] in which this stimulation principle was found to be very variable from one participant to the other. But interestingly, when introducing the elliptical motion of particles, the participants could distinguish the simulated button with a success rate of 95%. These figures illustrate that the elliptical motion of particles of the plate can indeed simulate a button click.

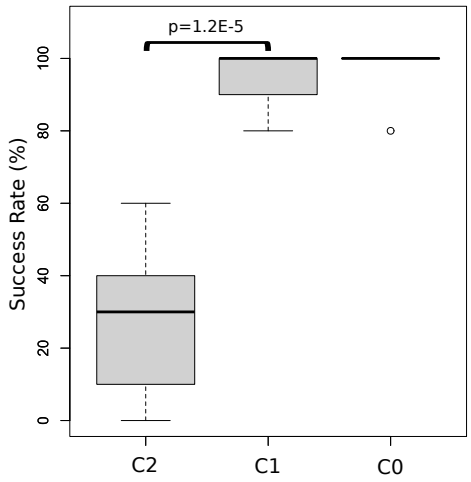

Figure 13: Experimental results: Success rate, computed for different conditions. The error bars, the whisker boxes and the horizontal bars show respectively the min. and max. values, their interquartile range and the median value.

	Condition		
	C2	C1	C0
Median Success (%)	30	100	100
Std	19.11	8.49	6.32

Table 1: Experimental results:success rate for different Λ

5. Conclusion

In this paper we proposed and implemented an new controller which can control simultaneously the vibration amplitude and the relative phase of two modes, one longitudinal and one transverse, and outside their resonant frequency. The performances were measured on an actual device, and presented a $2ms$ response time, and was robust besides external disturbances or the working frequency. The methodology, carried out in the (d,q) reference frame, also helped to estimate the parameters of the system used to design the controllers. Finally, the device is used to simulate a button. For that purpose, we conducted an psycho physic study which demonstrates that using the elliptical motion of particles produced by the synchronization of the aforementioned modes greatly improves the key click perception. The proposed design is suitable to produce virtual button on a rectangular device. Further work will focus on how to generate the elliptical motion on larger area.

Acknowledgement

This work has been carried out with the support of the IRCICA (Research Institute on software and hardware devices for information and Advanced com-

munication, USR 3380).

References

[1] Basdogan, C., Giraud, F., Levesque, Vi., Choi, S. : A Review of Surface Haptics: Enabling Tactile Effects on Touch Surfaces. IEEE Transactions on Haptics. 13 450–470 (2020)

[2] Park, G., Choi, S., Hwang, K., Kim, S., Sa, J., Joung, M.: Tactile effect design and evaluation for virtual buttons on a mobile device touchscreen. In: Proceedings of the 13th MobileHCI conference. p. 11–20 (2011)

[3] Hudin, C., Panëels, S.: Localisation of vibrotactile stimuli with spatio-temporal inverse filtering. In: Haptics: Science, Technology, and Applications. pp. 338–350. Springer International Publishing, Cham (2018)

[4] Emgin, S.E., Aghakhani, A., Sezgin, T.M., Basdogan, C.: Haptable: An interactive tabletop providing online haptic feedback for touch gestures. IEEE Transactions on Visualization and Computer Graphics **25**(9), 2749–2762 (Sep 2019)

[5] Monnoyer J., Diaz E., Bourdin C. and Wiertlewski M.: Perception of Ultrasonic Switches Involves Large Discontinuity of the Mechanical Impedance. In: IEEE Transactions on Haptics, vol. 11, no. 4, pp. 579–589 (2018)

[6] Gueorguiev, D., Kaci, A., Amberg, M., Giraud, F., Lemaire-Semail, B.: Travelling ultrasonic wave enhances keyclick sensation. In: Haptics: Science, Technology, and Applications. pp. 302–312. Springer International Publishing, Cham (2018)

[7] Ghenna, S., Vezzoli, E., Giraud-Audine, C., Giraud, F., Amberg, M., Lemaire-Semail, B.: Enhancing variable friction tactile display using an ultrasonic travelling wave. IEEE Transactions on Haptics **10**(2), 296–301 (April 2017)

[8] Garcia P., Giraud F., Lemaire-Semail B., Rupin M., Amberg M. (2020) 2MoTac: Simulation of Button Click by Superposition of Two Ultrasonic Plate Waves. EuroHaptics 2020. , in: I. Nisky, J. Hartcher-O'Brien, M. Wiertlewski, J. Smeets (Eds.), Haptics: Science, Technology, Applications, Springer International Publishing, Cham, 2020: pp. 343–352.

[9] S. Davis, I. Bucher, Automatic vibration mode selection and excitation; combining modal filtering with autoresonance, Mechanical Systems and Signal Processing. 101 (2018) 140–155.

[10] Giraud, F., Giraud-Audine, C.: Piezoelectric Actuators: Vector Control Method. Butterworth-Heinemann (2019)